

DISCLAIMER

This report was prepared as an account of work sponsored by an agency of the United States Government. Neither the United States Government nor any agency thereof, nor any of their employees, makes any warranty, express or implied, or assumes any legal liability or responsibility for the accuracy, completeness, or usefulness of any information, apparatus, product, or process disclosed, or represents that its use would not infringe privately owned rights. Reference herein to any specific commercial product, process, or service by trade name, trademark, manufacturer, or otherwise does not necessarily constitute or imply its endorsement, recommendation, or favoring by the United States Government or any agency thereof. The views and opinions of authors expressed herein do not necessarily state or reflect those of the United States Government or any agency thereof.

**Effects of Catalytic Mineral Matter on CO/CO₂ Ratio,
Temperature and Burning Time for Char Combustion**

Prof. John P. Longwell
Prof. Adel F. Sarofim
Prof. Ezra Bar-Ziv (Visiting Scientist)

Chun-Hyuk Lee

Quarterly Progress Report No. 3

April - June 1990

Prepared for

U.S. Department of Energy
Pittsburgh Energy Technology Center
Pittsburgh, Pennsylvania
Technical Project Officer - Philip M. Goldberg
Grant No. DE-FG22-89PC89774

by

Massachusetts Institute of Technology
Department of Chemical Engineering
Cambridge, MA 02139

MASTER

EP

Introduction

The high temperature oxidation of char is of interest in a number of applications in which coal must be burned in confined spaces. These include: the conversion of oil-fired boilers to coal using coal-water slurries, the development of a new generation of pulverized coal-fired cyclone burners, the injection of coal into the tuyeres of blast furnaces, the use of coal as a fuel in direct-fired gas turbines and in large-bore low-speed diesels, and entrained flow gasifiers. In addition there is a need to better understand the temperature history of char particles in conventional pulverized-coal-fired boilers in order to better understand the processes governing the formation of pollutants and the transformation of mineral matter.

The temperature of a char particle burning in an oxygen containing atmosphere is the product of a strongly coupled balance between particle size and physical properties, heat transfer from the particle, surface reactivity, CO_2/CO ratio and gas phase diffusion in the surrounding boundary layer and within the particle. In addition to its effects on burning rate, particle temperature has major effects on ash properties and mineral matter vaporization. Measurements of the temperature of individual burning char particles have become available in recent years and have clearly demonstrated large particle-to-particle temperature variations which depend strongly on particle size and on particle composition. These studies, done with pulverized coal, do not allow direct determination of the CO_2/CO ratio produced at the char surface or the catalytic effects of mineral matter in the individual char particles and it has generally been assumed that CO is the only product of the carbon-oxygen reaction and that CO_2 is formed by subsequent gas phase reaction. More recent

work, however, has pointed out the need to take CO₂ production into consideration in order to account for observed particle temperatures.

The importance of the CO₂/CO ratio of carbon oxidation products is illustrated by examination of the heats of reaction for formation of these products



The heat released by formation of CO₂ is a factor of 3.5 higher than for CO so the temperature of a particle will depend strongly on the CO₂/CO ratio produced. If gas diffusion through the boundary layer is fast, increased direct production of CO₂ produces a higher temperature and a higher burning rate. If the supply of oxygen to the surface is limited by diffusion through the boundary layer, production of CO₂ consumes half as much carbon as production of CO so carbon consumption rate is reduced even though temperature may be somewhat higher. Models of these complex interactions have been developed; however, the CO₂/CO ratio produced by the carbon-oxygen reaction must, at present be assumed or inferred from measurement of particle temperature.

CO₂/CO ratios can be strongly influenced by catalytic material in the carbon and by the char temperature. In this program we are measuring the CO₂/CO ratio for both catalyzed and uncatalyzed chars over a wide range of temperature. These results will then be used to develop predictive models for char temperature and burning rates.

Measurements of CO₂/CO ratio for an uncatalyzed char (spherocarb) were reported in the Oct-Dec 1989 progress report. This ratio varied from a maximum of 1.5 at 700 K and 100% oxygen to 0.06 at 1430 K and 5% oxygen.

In the Jan-March 1990 progress report results of kinetic modeling of the effect of temperature on this ratio were reported. The model results for uncatalyzed char corresponded closely to the experimental results. For catalyzed char, a substantial increase in CO_2/CO ratio was predicted. Progress on construction of the upgraded electrodynamic balance was also reported.

In this report we discuss the design and performance of an improved particle position control system and the improvements in measurement of particle surface area resulting from a combination of the high pressure capability and improved particle position control in our upgraded EDTGA.

RESULTS

A. Improved Particle Position Control System

The improved control system for the electrodynamic chamber is based on a development of Bar-Ziv et al., 1990, and Bar-Ziv and de Botton, 1990. Details of the electrodynamic chamber are given by Spjut, et al., 1986, and Bar-Ziv, et al., 1989. This position control system comprises three parts:

- (1) An electro-optical sensing system.
- (2) A data acquisition system and an on-line tracing algorithm that determines the particle position.
- (3) A PID controller.

The schematic of the system is shown in Fig. 1. A laser beam passes horizontally through the center of an electrodynamic chamber (through holes in the ring electrode) then traverses a diverging lens and finally is projected onto a linear photo diode array (PDA) that was placed vertically. The diameter of the laser beam, about 2 mm, is large enough

to follow a particle 100-200 μm in diameter throughout a displacement of 10 to 20 particle diameters. The magnification of the particle image was selected to cover 10-30% of the array depending on the maximum particle displacement to be controlled. Without a particle blocking the beam, all photodiodes were saturated to obtain maximum contrast between the shadow of the particle and the illuminated area. A 128 Reticon PDA was used with a sample and hold board. The scanning rate of the PDA was 1500-2000 Hz. The signal from the PDA was transferred through a 50-125 kHz A/D converter to the computer.

The computer serves as the tracing device and the controller. The signal from the PDA (after passing through the sample and hold board) was fed continuously into the analog to digital converter and was transferred directly to the computer memory. A tracing algorithm determined the particle position every three consecutive PDA scans, then a control algorithm provided a value to be fed back to the system by a D/A converter. The analog output signal was split, where one signal was inverted to a negative value. The two signals were fed into Analog Device operational amplifiers model 171J and then to the two end-caps of the electrodynamic chamber. With a 25-33 MHz 386-microprocessor the position control system is capable of sampling at 500-800 Hz. The major advantages of this system are (1) elimination of specific devices, digital or analog, for the position control system and (2) flexibility in the operation of the system since it is based on software rather than hardware.

We used a PID controller to rebalance the particle, expressed by

$$f_c = -g[z_n + \frac{1}{t_i} (\sum_n z_n)\Delta t + \frac{t_d}{\Delta t} (z_n - z_{n-1})] \quad (1)$$

where f_c is a signal to be fed back by the D/A converter, z_n is error position which is simply the position of the particle from the center of the chamber, determined for the n -th scanning, g is the gain (given in voltage per unit distance, t_i and t_d are the characteristic time for the integral and derivative parts, respectively, and Δt is the sampling time.

A convenient method for determining the optimal value of the PID terms is by solving the equation of motion with a PID control term. The next section deals with the equation of motion.

To determine the ultimate gain, a constant perturbation was imposed as a change in the DC voltage ($h \neq 0$). The ultimate gain was found from the simulation by assuming $t_d = 0$ and $t_i = \infty$ and varying the value of G until a steady state oscillation of the error was found. This value was then introduced into the P-controller and the position of the particle was measured. Synthetic char particles of about $140 \mu\text{m}$ diameter were used in this study. The AC frequency was usually 32 Hz. The value for the ultimate gain was found $G=0.4$. It is interesting to note that the ultimate frequency is equal to half the AC field frequency.

The working value for the gain was set to $G=0.24$ (60% gain is normally taken as the optimal proportional gain). The derivative characteristic time was varied until an optimal operation condition was found to equal $t_d=6.28$ (equal to the period for the ultimate conditions). The derivative term prevents the undershooting of the particle's motion. The integral characteristic time was varied for optimal operation was found to equal $t_i=12.56$ (four times the period time of the AC field alternation). The integral term relaxes the particle to the center with a characteristic time of about 100 ms.

B. Determination of Surface by CO₂ Adsorption-Desorption

We have extended our recently reported method for determining the surface area of single microporous particles, Dudek et al., 1989 using an electrodynamic chamber (EDC) by increasing the operating pressures from 1 at to 25 at. The value of total surface area is determined from adsorption measurements of CO₂ assuming mono-layer adsorption.

The total surface area of the particle is then calculated by

$$S_{tot} = \frac{x_s N_o \sigma_{CO_2}}{M_{CO_2}} \quad (3)$$

where σ_{CO_2} is the cross-sectional area of a CO₂ molecule. M_{CO_2} is the molecular weight of CO₂. N_o is Avogadro's number, and x_s is the ratio of CO₂ weight adsorbed at saturation to particle initial weight. Walker and Kini, 1965, provided the data base for the cross-sectional area of the CO₂ molecule.

The value of x_s estimated by extrapolation from the Dubinin-Polanyi model for microporous particles, yielding the following equation

$$\log(x) = \log x_s - \frac{\beta T}{\beta} \log^2\left(\frac{P_o}{P}\right) \quad (4)$$

where x is the ratio of CO₂ weight adsorbed to particle initial weight at partial pressure P of CO₂, P_o is the saturation vapor pressure of CO₂, T is temperature, β is the affinity coefficient of CO₂ relative to N_o , and β is a constant. From a plot of $\log(x)$ as a function of $\log^2(P_o/P)$ the value of x_s can be determined.

Alternatively, the value of x_2 can also be extrapolated from the Langmuir theory, Carberry, 1976, that relates the adsorbed weight fraction of CO_2 with its partial pressure by

$$x = x_2 \frac{(k_{\text{ads}}/k_{\text{des}})P}{1 + (k_{\text{ads}}/k_{\text{des}})P} \quad (5)$$

where k_{ads} and k_{des} are the rate coefficients for adsorption-desorption respectively. A plot of $1/x$ vs. $1/P$ should yield a linear behavior from which the values of x_2 and K_p can be determined ($K_p = k_{\text{ads}}/k_{\text{des}}$ is the adsorption-desorption equilibrium coefficient).

In the EDC we can measure the quantity x continuously. Figure 3 shows typical results of adsorption of CO_2 by a Sphero carb particle plotted as $1/x$ vs. $1/P$ at 25 °C. From a linear regression of the results of Fig. 2, the values for x_2 (from the intercept) and K_p (from the slope) were determined as 0.310 ± 0.008 and 0.378 ± 0.012 at atm^{-1} respectively (the error bars relate to one standard deviation). In this case the particle weight was about 1 μg .

Figure 3 shows the results of Fig. 2 in a Dubinin-Polanyi representation plotted as $\log(x)$ vs. $\log^2(P_0/P_{\infty 2})$. The value of P_0 was taken from Weast, 1976, $P_0 = 48250$ torr at 25°C. The value of the intercept was found -0.492 ± 0.003 equivalent to $x_2 = 0.321 \pm 0.003$. The discrepancy between the two methods for extrapolating the value of x_2 is about 3%.

To calculate the total surface area the cross sectional area of CO_2 was taken as 24.2 \AA^2 . The total surface area the cross sectional area of CO_2 was taken as 24.2 \AA^2 . The total surface area of this particle was found $1070 \pm 20 \text{ m}^2/\text{g}$ (the particle was $155 \mu\text{m}$ in diameter with apparent density of 0.6 g/cm^3).

Measurements of CO₂ desorption were also carried out to yield a point to point difference from the adsorption measurements of about 1%. Adsorption-desorption cycles were carried out for 10 particles to yield a scatter of less than 5% in the measured value for saturation adsorption.

The major advantage of using high pressure measurements for evaluating the saturation value for CO₂ adsorption is the improved accuracy of the extrapolation procedure. Previous measurements with the EDC at atmospheric pressure, Dudek, et al., 1989, yielded values for the surface area for similar particles of comparable value with a relative error of about 15%. The results of the high pressure measurements are however bounded with an error of about 3%. Also, the equilibrium adsorption-desorption coefficient was found with a high accuracy, whereas from atmospheric measurements it was not practical to obtain an accurate value.

Future Program

During the next quarter it is anticipated that construction of the upgraded electrodynamic TGA will be sufficiently advanced to allow initiation of oxidation experiments.

These will include:

- o Oxidation of uncatalyzed spherocarb to establish correspondence with the results of the first quarter work.
- o Oxidation of spherocarb catalyzed with calcium or iron. Critical temperature for charge loss will be determined followed by measurements of CO₂/CO ratio and oxidation rate.

References

Bar-Ziv, E., and de Botton, G., "The Motion of a Charged Particle in an Electrodynamic Chamber under Feedback Control," Aeros. Sci. Tech., in press.

Bar-Ziv, E., de Botton, G., Bar-Ziv, R.H., Martsiano, Y., and Ben-Dor, G., "The Motion of a Charged Particle in an Electrodynamic Chamber," Aeros. Sci. Tech., in press.

Bar-Ziv, E., Jones, D.B., Spjut, R.E., Dudek, D.R., Sarofim, A.F. and Longwell, J.P., Combustion and Flame 75, 81-106 (1989).

Carberry, J.J. Chemical and Catalytic Reactions Engineering; Chemical Engineering Series; McGraw-Hill: London, 1976.

Dudek, D.R.; Longwell, J.P.; Sarofim, A.F. Energy and Fuels 1989, 3, 24.

Spjut, R.C.; Bar-Ziv; Sarofim, A.F.; Longwell, J.P. Rev. Sci. Instrum. 1986. 57, 1604.

Walker, P.L., Jr.; Kini, K.A. Fuel 1965, 44, 453.

Weast, R.C., Ed. Handbook of Chemistry and Physics, CRC 1975, 56th edition.

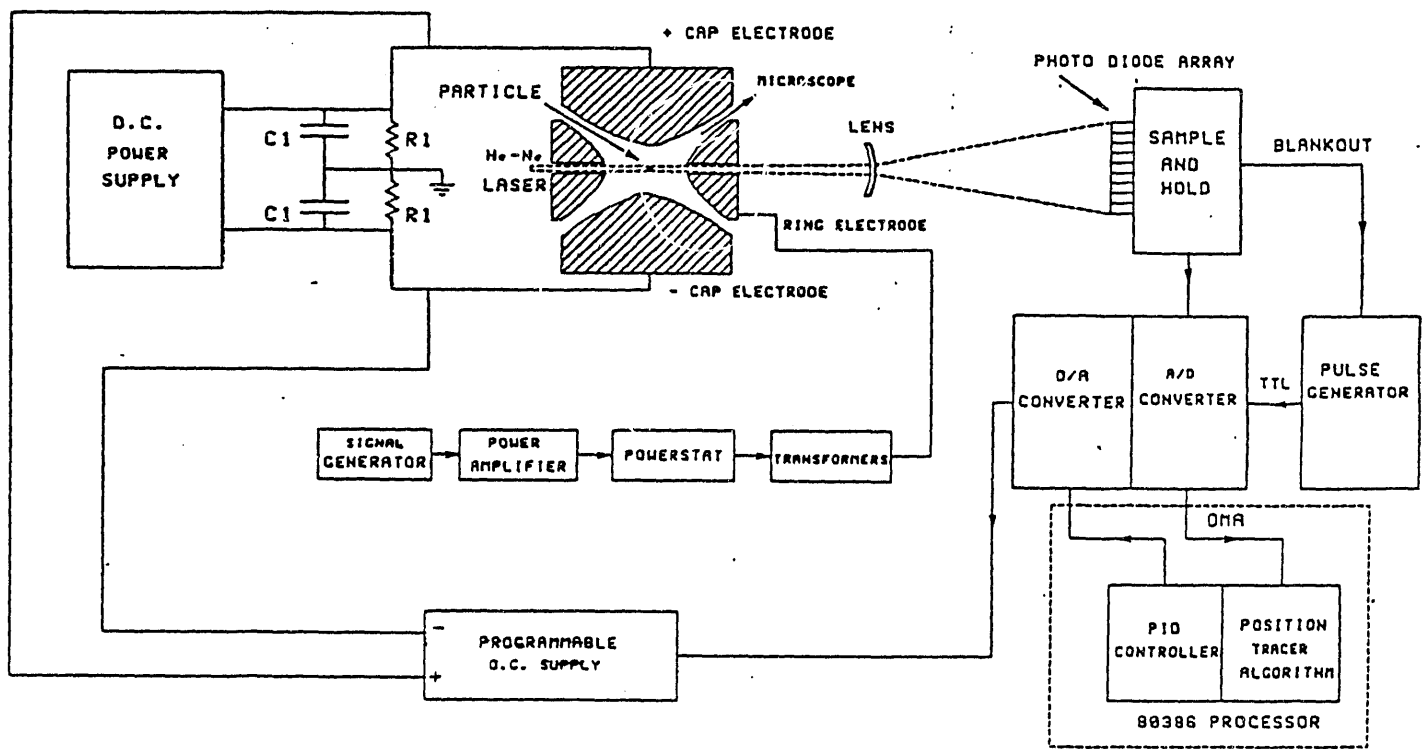


Figure 1. The Schematic of a Position Control System Based on Photodiode Array Shadowgraphy.

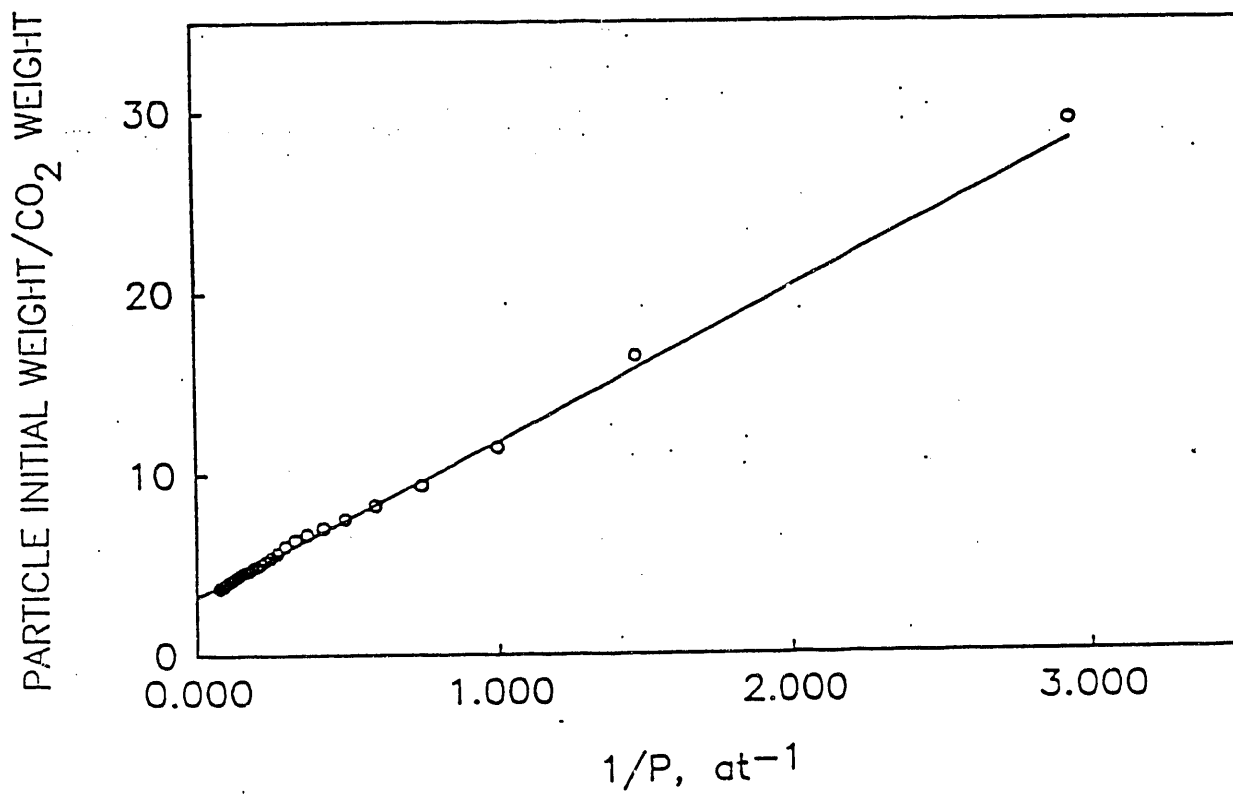


Figure 2 The Inverse Weight Fraction $1/x$ of CO_2 Adsorbed by a $155 \mu\text{m}$ diameter Sphero carb Particle as a Function of the Inverse Partial Pressure of CO_2 Partial Pressure P at 25°C . (Circles represent experimental data, solid line the best fit).

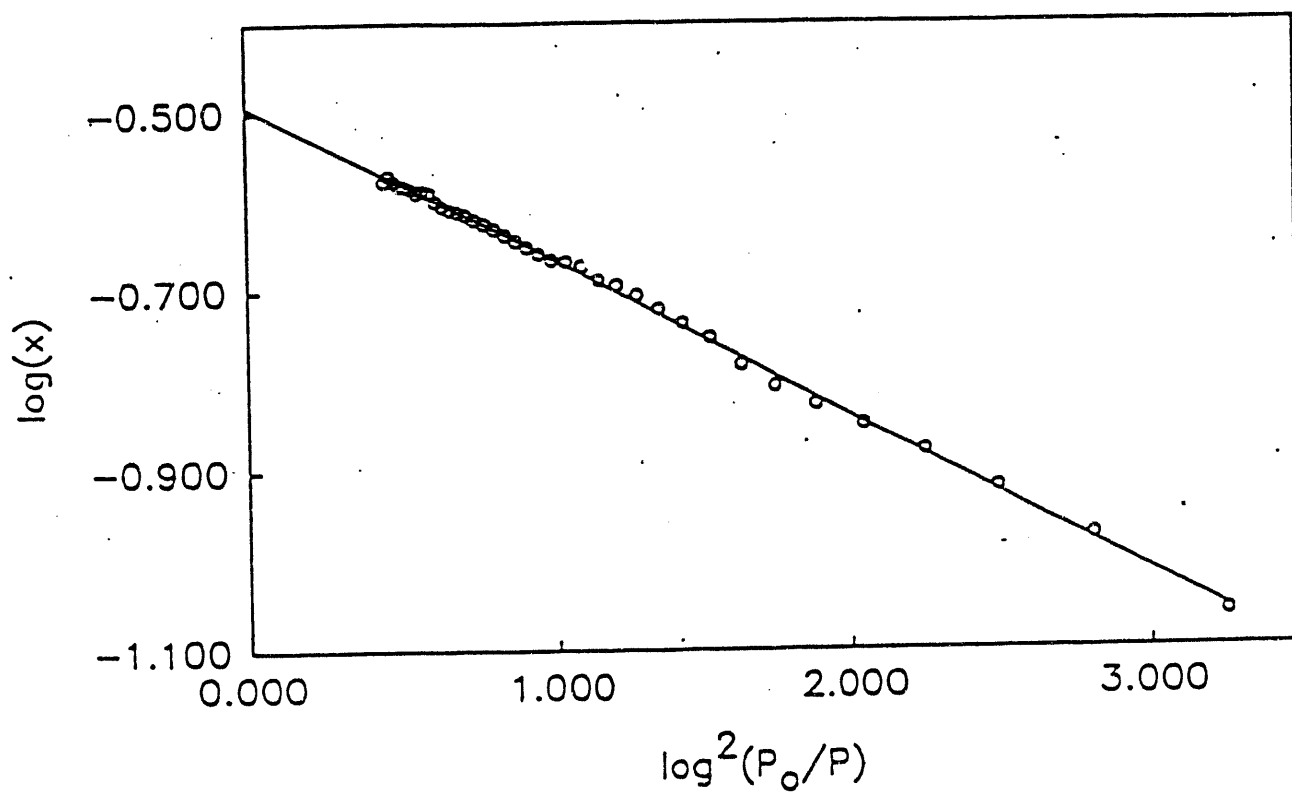


Figure 3 Results of Fig. 3 plotted according to the Dubinin-Polanyi equation as $\log(x)$ vs. $\log^2(P_0/P)$.

END

**DATE
FILMED**

4 / 6 / 93

